

Maximally-localized Wannier functions for disordered systems: application to amorphous silicon

Pier Luigi Silvestrelli,¹ Nicola Marzari,² David Vanderbilt,² Michele Parrinello¹

¹*Max-Planck-Institut für Festkörperforschung, Heisenbergstr. 1, 70569 Stuttgart, Germany*

²*Department of Physics and Astronomy, Rutgers University, Piscataway, NJ 08854-8019, USA*

(April 2, 1998)

We use the maximally-localized Wannier function method to study bonding properties in amorphous silicon. This study represents, to our knowledge, the first application of the Wannier-function analysis to a disordered system. Our results show that, in the presence of disorder, this method is extremely helpful in providing an unambiguous picture of the bond distribution. In particular, defect configurations can be studied and characterized with a novel degree of accuracy that was not available before.

Keywords: A. disordered systems, A. semiconductors, C. point defects, D. electronic states (localized).

I. INTRODUCTION

Since their introduction in 1937 Wannier functions¹ have played an important role in the theoretical study of the properties of periodic solids. Moreover the representation of the electronic ground state of periodic systems in terms of localized Wannier or Wannier-like orbitals has recently attracted considerable attention due to the development of “order-N” methods² and to the formulation of the modern theory of electronic polarization³. In the case of finite systems, localized orbitals are widely used to describe and understand chemical concepts such as bonds, lone-pair orbitals, and valence-electron charge distributions; different criteria^{4–6} have been developed for producing optimum localized orbitals.

In periodic systems the determination of localized orbitals or Wannier functions is much less trivial^{7,8}. Recently, Marzari and Vanderbilt⁸ developed a very practical method for generating maximally-localized Wannier functions starting from the knowledge of the occupied Bloch states. This amounts to the generalization for periodic systems of the Boys’ localized-orbital method⁵ that is commonly used in quantum chemistry. The new technique has been successfully applied to crystal systems and small molecules⁸. Here we apply for the first time the same procedure to a disordered system, namely amorphous silicon. We show that, also in this case, the Wannier functions are extremely useful in providing a clear description of the relevant electronic and bonding properties. They also help in eliminating many of the ambiguities that are usually associated with identifying defects in a disordered system.

II. METHOD

The Wannier functions¹ are defined in terms of a unitary transformation of the occupied Bloch orbitals. Even for the case of a single band, the Wannier functions are not uniquely defined, due to the arbitrary freedom in the

phases of the Bloch orbitals. In the multiband case this freedom becomes more general, and includes the choice of arbitrary unitary transformations among all the occupied orbitals at every point in the Brillouin zone (BZ). Marzari and Vanderbilt⁸ resolve this indeterminacy by requiring that the total spread of the Wannier functions

$$S = \sum_n \left(\langle r^2 \rangle_n - \langle \mathbf{r} \rangle_n^2 \right), \quad (1)$$

be minimized in real space, in analogy with Boys’⁵ criterion for finite systems. In Eq. (1) $\langle \dots \rangle_n$ indicates the expectation value with respect to the n -th Wannier function $w_n(\mathbf{r})$. Marzari and Vanderbilt⁸ have discussed how to properly define the operators \mathbf{r} and r^2 in a periodic system and have detailed the procedure to determine the functions $w_n(\mathbf{r})$ for a general k -point sampling of the BZ. Since we have in mind applications to large and disordered systems, we restrict ourselves here to the case of Γ -point only sampling of the BZ.

Our optimization procedure is closely related to that described in Appendix A of Ref. 8. We report explicitly the formulas to be used in a calculation with a cubic supercell of side L , which is the case of our simulation. The minimum spread criterion of Eq. (1) is equivalent to the problem of maximizing the functional

$$\Omega = \sum_n (|X_{nn}|^2 + |Y_{nn}|^2 + |Z_{nn}|^2), \quad (2)$$

where $X_{mn} = \langle w_m | e^{-i\frac{2\pi}{L}x} | w_n \rangle$. Similar definitions for Y_{mn} and Z_{mn} apply. Maximization of Ω is performed using a steepest descent (SD) algorithm. We start the procedure by constructing the new matrices $X^{(1)}$, $Y^{(1)}$ and $Z^{(1)}$ via the unitary transformations $X^{(1)} = \exp(-A^{(1)})X^{(0)}\exp(A^{(1)})$ (and similarly for $Y^{(1)}$ and $Z^{(1)}$), where $X_{mn}^{(0)} = \langle w_m^{(0)} | e^{-i\frac{2\pi}{L}x} | w_n^{(0)} \rangle$ and $w_n^{(0)}(\mathbf{r}) = \psi_n(\mathbf{r})$ are the Kohn-Sham (KS) orbitals obtained after a conventional electronic structure calculation. $A^{(1)}$ is an antihermitian matrix corresponding to a

finite step in the direction of the gradient of Ω with respect to all the possible unitary transformations given by $\exp(-A)$: $A^{(1)} = \Delta t (d\Omega/dA)^{(0)}$, where Δt is the conventional SD “time-step”. The gradient $d\Omega/dA_{mn}$ is given by the sum of $[X_{nm}(X_{nn}^* - X_{mm}^*) - X_{mn}^*(X_{mm} - X_{nn})]$ and the equivalent terms with Y and Z substituted in place of X . The process is repeated for many SD iterations up to convergence in the Ω functional. The maximally-localized Wannier functions are then given by $w_n(\mathbf{r}) = \Pi_i \exp(-A^{(i)})\psi_n(\mathbf{r})$. The coordinate x_n of the n -th Wannier-function center (WFC) is computed using the formula

$$x_n = -\frac{L}{2\pi} \text{Im} \ln \langle w_n | e^{-i\frac{2\pi}{L}x} | w_n \rangle, \quad (3)$$

with similar definitions for y_n and z_n . Eq. (3) has been shown by Resta⁹ to be the correct definition of the expectation value of the position operator for a system with periodic boundary conditions. The computational effort required in Eqs. (2) and (3) is negligible, once the scalar products needed to construct the initial $X^{(0)}$, $Y^{(0)}$ and $Z^{(0)}$ have been calculated.

III. RESULTS AND DISCUSSION

Amorphous silicon has been one of the first systems studied¹⁰ with the Car-Parrinello molecular dynamics method¹¹. We analyse here some selected configurations taken from a molecular-dynamics simulation performed by Chiarotti¹². These configurations have been obtained by quenching from the liquid state a sample of 64 Si atoms, contained in a cubic supercell of side 10.86 Å and periodically repeated in space. The total length of the simulation run was about 10 ps. Since our study is based on the local density approximation (LDA) to density-functional theory (DFT), each orbital is occupied twice and unpaired spin defects cannot be observed. However, such defects are expected to have a low density, as suggested by electron spin resonance experiments¹³.

In amorphous silicon most of the atoms are tetrahedrally bonded (sp^3 hybridized); however different kinds of defects can be present and have been proposed in the literature^{10,14–17}: twofold coordinated atoms forming spinless, neutral defects; threefold coordinated atoms with neutral or charged dangling bonds; fourfold coordinated atoms characterized by stretched (“weak”) bonds and by bond angles that are rather far from the tetrahedral angles; and fivefold coordinated atoms (“floating bonds”).

The usual analysis of the bonding properties is based on the coordination number, i.e. the number of atoms lying inside a sphere of a chosen radius r_c centered on the selected atom. Such a simplified structural analysis is sensitive to the value chosen for r_c . More importantly, it is also completely blind to the electronic charge distribution, which ought to be important to any description of

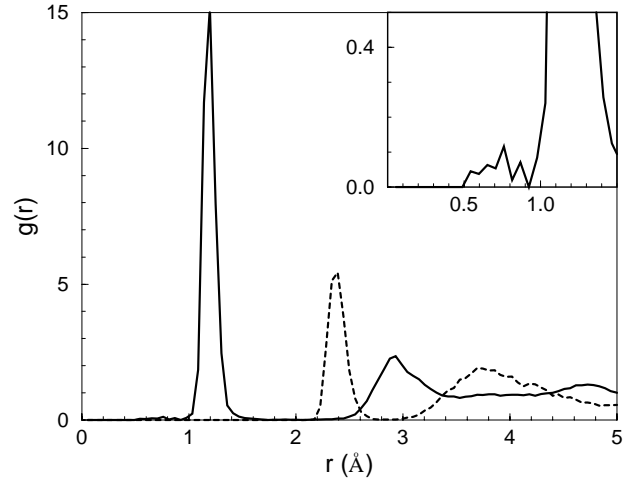


FIG. 1. Si-Si (dashed line) and Si-WFC (solid line) pair correlation functions. The detailed structure, in the range 0.0–1.5 Å, is shown in the inset. The data have been obtained by averaging over 17 configurations of the MD simulation.

chemical bonding. Analysis of the full charge distribution and bonding in terms of the Wannier functions is rather complex. However, as we show below, the knowledge of the positions of the WFCs suffices to capture most of the chemistry of the system and to identify its defects.

The ionic structure of a disordered system is best described in terms of correlation functions. We treat here the centers of the localized Wannier functions as a second species of classical particles, and we regard amorphous silicon as a statistical assembly of these two kinds of particles, the Si ions and the WFCs. In Fig. 1 we show $g(r)$, the standard Si-Si pair correlation function, together with $g_w(r)$, the Si-WFC pair correlation function. As can be seen, $g(r)$ and $g_w(r)$ exhibit strong peaks at $\simeq 2.4$ and at $\simeq 1.2$ Å, respectively, thus indicating that the electronic charge is mostly localized in the middle of the Si-Si bonds, as expected in a covalent-bonded system. The spread in the peaks indicates the disorder-induced strain in the Si-Si bond. However, $g_w(r)$ shows some structure also for values of r in the range 0.5–1.0 Å (see inset). This means that a few WFCs are anomalous in being very close to the Si ions. This behaviour represents a clear indication of the presence of defects in the system.

If the coordination number is computed by integration of $g(r)$ up to $r_c = 2.80$ Å (the position of the first minimum), we find that, on average, 96.5 % of the Si ions are fourfold coordinated, while 3.5 % are fivefold coordinated. Therefore, according to an analysis restricted to the ionic coordinates alone, all defects in the system are identified as fivefold-coordinated Si ions. This is in agreement with the findings of previous ab-initio simulations¹⁰. However, when we choose a coordination criterion based on the Wannier function representation, we get rather different results. We will say that a bond exists between two Si ions when they share a common

WFC located within $r_w = 1.75$ Å of each ion, r_w being the position of the first minimum of $g_w(r)$. With this convention, we find that 97.5 % of the Si ions are fourfold bonded; of the remaining ions, only ~ 0.6 % have 5 bonds, while the others are more or less equally subdivided into twofold-bonded and threefold-bonded ions. Therefore, although the total density of defective atoms that we obtain is similar to that coming from the bare coordination analysis, the nature of the defects appears to be different.

This fact is best illustrated by looking at the bonds formed among a few ions, in selected configurations of the molecular-dynamics simulation. In Fig. 2(a) ion A is fivefold coordinated and has 5 bonds, while ion B is fourfold coordinated but has 3 bonds only. In fact no WFC is found between ion B and ion C. Notice that the bond between ion A and ion B is somehow anomalous since the distance from the corresponding WFC to ion B is considerably smaller than to ion A (0.87 and 1.56 Å respectively), and the A-B bond appears to be distorted. As the ions move, the electronic configuration also changes, and in fact we find that after about 10 ps the WFC located between ion A and ion B comes still closer to ion B (see Fig. 2(b)). The distance is reduced to 0.57 Å, in such a way that the A-B bond is broken or at least severely weakened. In this configuration, according to our criterion, ion A is fourfold bonded, while ion B has only 2 bonds. Interestingly, the twofold-bonded atom was proposed by Adler¹⁵ as the lowest-energy defect in amorphous silicon. The defect we observe in Fig. 2(b) probably represents a transient state in which ion B breaks the bond with ion A and tries to form a new bond with a different nearest-neighbour, possibly ion C. This conclusion is supported by the fact that the direction of the vector connecting ion B to the anomalous WFC is intermediate between the B-A and B-C directions. Further confirmation comes from inspection of the isosurface of the electronic charge distribution associated with the anomalous Wannier function. Notice that the density profile of this Wannier function is different from the one associated with a normal covalent bond, as shown in Fig. 2(a). To determine whether a new bond with ion C is really formed or whether the configuration of ion B in Fig. 2(b) is stable would require a longer simulation, which is beyond the scope of the present work.

We stress again that the interesting transformation in the bonding properties of ions A and B, which we have described using the Wannier function analysis, cannot be detected using the simple coordination number criterion. In fact, in the configuration of Fig. 2(b), the coordination numbers of ion A and B are the same as in the configuration of Fig. 2(a), although the A-B distance is significantly increased from 2.38 to 2.59 Å.

The Wannier function analysis allows a description of the electronic charge distribution in terms of well-defined, localized functions; the clear representation of the bonding properties of the system based on the positions in real space of the WFCs can then be followed by a more

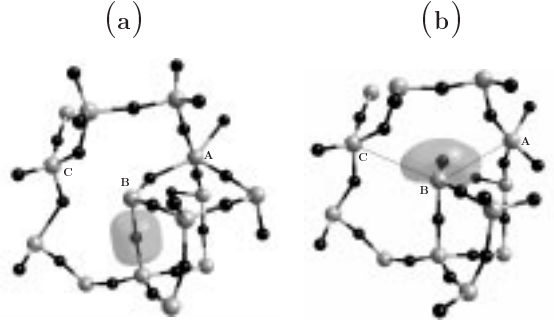


FIG. 2. Snapshots of 2 different configurations of the MD simulation of amorphous silicon. Large grey balls denote Si ions, while small black balls denote WFCs. A, B and C label the Si ions, whose bonding properties are discussed in the text. For clarity only the Si ions and WFCs lying within 4 Å of ion B are shown. We also plot the isosurface densities $\rho_n(\mathbf{r}) = |w_n(\mathbf{r})|^2$ corresponding to a normal covalent Wannier function in (a), and to an anomalous Wannier function close to ion B in (b). Thin lines in (b) indicate directions of possible bonds of ion B with ions A and C.

quantitative study. For instance, one can relate specific features of the electronic density of states to a particular Wannier function $w_n(\mathbf{r})$, defining a “projected density of states”

$$N_n(E) = \sum_m |\langle w_n | \psi_m \rangle|^2 \delta(E - E_m), \quad (4)$$

where ψ_m and E_m are the KS eigenvectors and eigenvalues. As can be seen from Fig. 3, the $N_n(E)$ function associated to the anomalous WFC of Fig. 2(b) exhibits a strong peak which matches the peak in the electronic density of states located above the valence-band edge. This peak can be associated with the highest-energy occupied KS state. We have therefore a clear example in which the electronic states of the structural defects present in our sample are introduced into the energy gap.

Another important advantage of the use of the Wannier functions is that a precise calculation of the localization degree of the electronic charge is possible, in contrast with previous approximate estimates^{10,17}. In fact one can easily compute the quantity

$$\sigma_n = \sqrt{\langle r^2 \rangle_n - \langle \mathbf{r} \rangle_n^2}, \quad (5)$$

which corresponds to the spread in real space of the Wannier function $w_n(\mathbf{r})$. Considering again the anomalous WFC of Fig. 2(b), we find that $\sigma_n = 1.94$ Å, a value significantly larger than the average spread obtained by considering all the WFCs, $\bar{\sigma} = 1.38$ Å. We find therefore that the Wannier function associated to the defect state is less localized than the Wannier functions associated to normal states. This interesting result confirms, in a quantitative way, the qualitative observation of Fedders, Drabold and Klemm¹⁷ who pointed out that the defect states can be far less localized than expected.

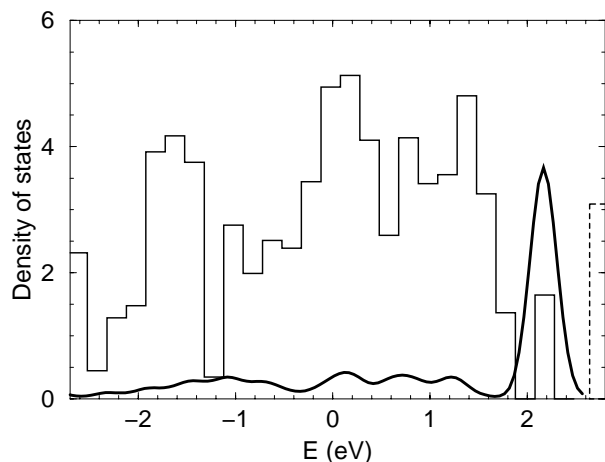


FIG. 3. Histogram of the electronic density of states (thin line, the dashed portion indicating the conduction band) compared with the projected density of states $N_n(E)$ (thick line) corresponding to the anomalous WFC of Fig. 2(b) (see text for definition). The histogram has relatively large fluctuations because only a single ionic configuration is considered. The curve $N_n(E)$ has been smoothed with a gaussian broadening.

IV. CONCLUSIONS

In conclusion, we have described a novel application of the Wannier function analysis to a disordered system. We have shown that a simple geometrical analysis of the positions of the WFCs is already sufficient to extract useful information about the bonding properties of the ions, particularly in those interesting defective configurations which, using traditional approaches, can only be studied in a very crude way. In addition, since in our method the localized Wannier functions are explicitly available, a quantitative analysis, which allows us to estimate accurately the degree of localization of the electronic charge, is possible. It also allows us to clarify the nature of the relevant features in the electronic density of states.

An additional advantage of the current approach of analyzing the dynamics of the system of ions plus WFCs is that it should be possible to extract information about the dipolar fluctuations, i.e. about the dielectric response function $\chi(\mathbf{k}, \omega)$. In fact the present approach is closely related to that of Ref.¹⁸ where, however, only the $k = 0$ response relevant to optical probes is computed, so that only the macroscopic polarization is needed at each time step. The current approach opens the possibility of extracting some local (i.e. k -dependent) information as well.

ACKNOWLEDGMENTS

We thank M. Boero and M. Bernasconi for useful discussions.

- ¹ G. H. Wannier, Phys. Rev. **52**, 1937, 191.
- ² G. Galli and M. Parrinello, Phys. Rev. Lett. **69**, 1992, 3547; F. Mauri, G. Galli, R. Car, Phys. Rev. B **47**, 1993, 9973; F. Mauri and G. Galli, *ibid.* **50**, 1994, 4316; P. Ordejón, D. Drabold, M. P. Grumbach, R. M. Martin, *ibid.* **48**, 1993, 14646; *ibid.* **51**, 1995, 1456; W. Kohn, Chem. Phys. Lett. **208**, 1993, 167; W. Hierse and E. B. Stechel, Phys. Rev. B **50**, 1994, 1781; J. Kim, F. Mauri, G. Galli, *ibid.* **52**, 1995, 1640; E. Hernández, M. J. Gillan, *ibid.* **51**, 1995, 10157; E. Hernández, M. J. Gillan, C. M. Goringe, *ibid.* **53**, 1996, 7147; P. Ordejón, E. Artacho, J. M. Soler, *ibid.* **53**, 1996, R10441.
- ³ R. D. King-Smith and D. Vanderbilt, Phys. Rev. B **47**, 1993, 1651; *ibid.* **48**, 1993, 4442; R. Resta, Rev. Mod. Phys. **66**, 1994, 899; G. Ortiz and R. M. Martin, Phys. Rev. B **49**, 1994, 14202; R. W. Nunes and D. Vanderbilt, *ibid.* **50**, 1994, 17611.
- ⁴ T. Sano, S. Narita, Y. J. I'Haya, Chem. Phys. Lett. **138**, 1987, 291; J. Pipek and P. G. Mezey, J. Chem. Phys. **90**, 1989, 4916; M. Couty, C. A. Bayse, M. B. Hall, Theor. Chem. Acc. **97**, 1997, 96.
- ⁵ S. F. Boys, *Quantum Theory of Atoms, Molecules, and the Solid State*, P.-O. Löwdin, ed. (Academic Press, New York, 1966), p. 253.
- ⁶ A. D. Becke, K. E. Edgecombe, J. Chem. Phys. **92**, 1990, 5397; A. Savin, A. D. Becke, J. Flad, R. Nesper, H. Preuss, H. G. von Schnering, Angew. Chem. **103**, 1991, 421; A. Savin, H.-J. Flad, J. Flad, H. Preuss, H. G. von Schnering, Angew. Chem. **104**, 1992, 185; B. Silvi, A. Savin, Nature, **371**, 1994, 683.
- ⁷ B. Sporkmann, H. Bross, Phys. Rev. B **49**, 1994, 10869; P. Fernandez, A. Dal Corso, A. Baldereschi, F. Mauri, Phys. Rev. B **55**, 1997, R1909; A. Shukla, M. Dolg, P. Fulde, H. Stoll, Phys. Rev. B **57**, 1998, 1471.
- ⁸ N. Marzari, D. Vanderbilt, Phys. Rev. B **56**, 1997, 12847.
- ⁹ R. Resta, Phys. Rev. Lett. **80**, 1998, 1800.
- ¹⁰ I. Štich, R. Car, M. Parrinello, Phys. Rev. B **44**, 1991, 11092.
- ¹¹ R. Car and M. Parrinello, Phys. Rev. Lett. **55**, 1985, 2471.
- ¹² G. L. Chiarotti, private communication.
- ¹³ W. G. Spitzer, G. K. Huber, T. A. Kennedy, Nucl. Instrum. Methods, **209/210**, 1983, 309.
- ¹⁴ P. W. Anderson, Phys. Rev. B **34**, 1975, 953.
- ¹⁵ D. Adler, Phys. Rev. Lett. **25**, 1978, 1755.
- ¹⁶ S. R. Elliott, *Physics of Amorphous Materials*, Longman, London, 1984.
- ¹⁷ P. A. Fedders, D. A. Drabold, S. Klemm, Phys. Rev. B **45**, 1992, 4048.
- ¹⁸ P. L. Silvestrelli, M. Bernasconi, M. Parrinello, Chem. Phys. Lett. **277**, 1997, 478; A. Debernardi, M. Bernasconi, M. Cardona, M. Parrinello, Appl. Phys. Lett. **71**, 1997, 2692.